

## Effect of acceleration and randomization in refined cellular automaton model and possible relation with synchronized flow

ZHAO Bo-han, HU Mao-bin, JIANG Rui, WU Qing-song

(School of Engineering Science, University of Science and Technology of China, Hefei 230026, China)

**Abstract:** The effect of acceleration  $a$  and randomization  $D$  in a refined Nagel-Schreckenberg traffic flow model is investigated. It is found that when  $a \geq D$ , there is no qualitative change of the fundamental diagram and spatiotemporal pattern. In contrast, when  $a < D$ , qualitative changes of traffic flow characteristics appear, and the congested traffic flow exhibits the characteristics of synchronized flow. Based on this finding, we study spatiotemporal patterns induced by an on-ramp, using the refined model with  $a < D$  and considering slow-to-start effect. It is shown the patterns are consistent with the results of three phase traffic theory. Our work is expected to shed some light on the mechanism of synchronized flow, which might be related to the value of  $a/D$ .

**Key words:** traffic flow; synchronized flow; cellular automaton model

**CLC Number:** U491 **Document Identification Code:** A **Paper Number:** 1671-5497(2009)Sup. 2-0097-06

The mechanism and physical characteristics of traffic flow have been investigated since 1950's<sup>[1]</sup>. For a mathematical description of freeway traffic flow, a mass of different macroscopic and microscopic models have been proposed and studied. Much progress has been made in understanding traffic features by using these traffic flow models. Besides, there are efforts to establish a link between macroscopic and microscopic models in order to find a universal feature.

In recent years, it has turned out that cellular automaton (CA) is a useful tool to simulate the complex non-linear large scale traffic flow<sup>[2-4]</sup>. In CA models, a road is divided into cells which can be either empty or occupied. The vehicles have integer velocity  $v = 0, 1, 2, \dots, v_{\max}$  and their velocities and positions are usually updated in parallel. In

1992, a well-known CA model was proposed by Nagel and Schreckenberg<sup>[5]</sup>. In Nagel-Schreckenberg (NaSch) model, each cell usually corresponds to 7.5 m and one time step corresponds to 1 s. As a result, the acceleration  $a$  and the randomization deceleration  $D$  correspond to 7.5 m/s<sup>2</sup>. The NaSch model is a minimal model and it could reproduce some basic traffic features, such as spontaneous formation of jams. However, this model is too simple to simulate many empirically observed spatiotemporal features of congested traffic patterns, such as synchronized flow, capacity drop, and traffic breakdown<sup>[6-7]</sup>.

In order to describe real traffic flow better, many other CA models have been presented. Nevertheless, the effect of acceleration  $a$  and randomization  $D$  on traffic dynamics has not been studied systematically. In this paper,

**Received:** 2009-05-20.

**Fund:** State Key Development Program for Basic Research of China (2006CB705500); National Natural Science Foundation of China (10532060, 70601026, 10672160, 10872194).

**Corresponding author:** HU Mao-bin (1978 -), male, associate professor. Research fields: complex networks, urban traffic. E-mail: humaobin@ustc.edu.cn

this effect is investigated by using a refined NaSch model, in which each cell corresponds to 1.5 m. It is found that when  $a \geq D$ , there is no qualitative change of the fundamental diagrams and the spatiotemporal patterns. In contrast, when  $a < D$ , qualitative changes of traffic flow characteristics appear, and the congested traffic flow exhibits the characteristics of synchronized flow. Based on this finding, we study spatiotemporal patterns induced by an on-ramp, using the refined model with  $a < D$  and considering slow-to-start effect. It is shown that the empirically observed traffic patterns could be reproduced.

### 1 Model

In the refined NaSch model used in our work, a road is divided into cells and each cell corresponds to 1.5 m. The parallel update rules of the model are as follows:

(1) Acceleration:

$$v_n(t+1) = \min(v_n(t) + a, v_{\max})$$

(2) Braking rule:

$$v_n(t+1) = \min(v_n(t+1), d_n)$$

(3) Randomization: With probability  $p$ ,

the velocity of vehicle  $n$  decreases by  $D$  units:

$$v_n(t+1) = \max(v_n(t+1) - D, 0)$$

(4) Car motion:

$$x_n(t+1) = x_n(t) + v_n(t+1)$$

Here vehicle  $n$  is moving behind vehicle  $n+1$ .  $v_n$  and  $x_n$  denote velocity and position of vehicle  $n$ .  $d_n = x_{n+1} - x_n - L_v$  is the space gap between vehicle  $n$  and vehicle  $n+1$ , where  $L_v$  is vehicle length and is supposed to be  $L_v=7.5$  m (5 cells).  $a$  represents acceleration of the vehicle and  $D$  is the randomization deceleration. In the refined model, one time step corresponds to 1 s. The range of  $a$  and  $D$  we are interested in is from 1 to 5. In other words, in the refined model, the maximum of acceleration and randomization deceleration is 5, which corresponds to  $7.5 \text{ m/s}^2$ , equaling to the acceleration and the randomization deceleration of the original NaSch model.

### 2 Simulation results on circular road

In this section, the simulations are performed on a single-lane circular road. Fig. 1 shows the fundamental diagrams with parameters  $a \geq D$ . It can be seen the diagrams only depend on the ratio  $a/D$ : the maximum flow rate increases with the increase of  $a/D$ . When  $a/D$  is fixed, the diagram is essentially independent of  $a$  and  $D$ . Fig. 2 compares the spatiotemporal patterns at density  $\rho=0.3$  at different values of  $a$  and  $D$  with  $a \geq D$ . It can be seen there is no qualitative change of patterns: the congested flow exhibits start-stop waves.

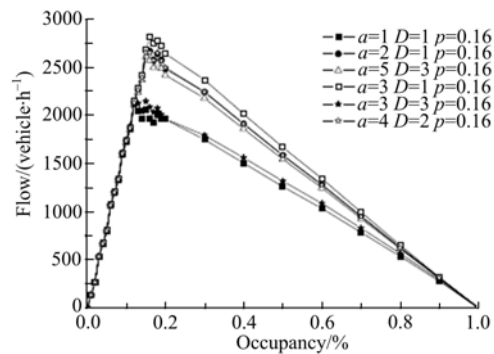
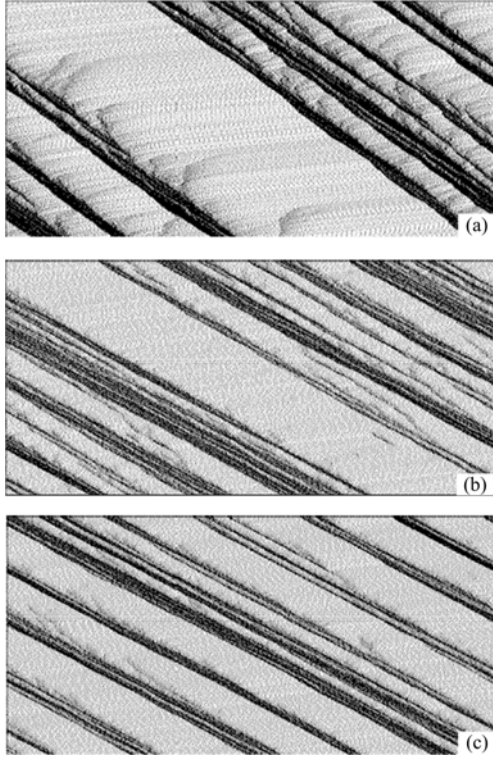


Fig. 1 Fundamental diagrams with parameters  $a \geq D$ . The road length  $L = 30$  km (20 000 cells).

Fig. 3 shows the fundamental diagrams with parameters  $a < D$ . One can see the diagrams do not solely depend on the ratio  $a/D$ , especially when  $a/D$  is small (see, e. g., the curve of  $a=1, D=2$  and the curve of  $a=2, D=4$ ). When  $a$  or  $D$  is fixed, the maximum flow rate decreases with the decrease of  $a/D$ . Fig. 4 compares the spatiotemporal patterns at density  $\rho=0.3$  at different values of  $a$  and  $D$  with  $a < D$ . It can be seen with the decrease of  $a/D$ , a qualitative change of traffic patterns appears. The jams gradually disappear and a macroscopic homogeneous congested flow gradually appears, which seems to exhibit the characteristics of synchronized flow.

Next we demonstrate the congested flow obtained at  $a < D$  is probably related to syn-



**Fig. 2** Spatiotemporal patterns at density  $\rho=0.3$  at different values of  $a$  and  $D$  with  $a \geq D$ . The road length  $L=7.5$  km (5000 cells). The randomization  $p=0.16$ . (a)  $a=1, D=1$ ; (b)  $a=5, D=3$ ; (c)  $a=4, D=2$ .

chronized flow. We focus on the parameter values  $a = 3, D = 5$ . It is known that in synchronized flow<sup>[8]</sup>, no long-range correlations exist in the autocorrelations of the density, average velocity, and flow rate, and the crosscorrelation function between density and flow rate vanishes in large time scale<sup>[9]</sup>. Fig. 5 shows the autocorrelation of the density, average velocity, and

$$a_x(\tau) = \frac{\langle x(t)x(t+\tau) \rangle - \langle x(t) \rangle^2}{\langle x^2(t) \rangle - \langle x(t) \rangle^2}$$

flow rate in congested flow shown in Fig. 4 (b). Here the brackets indicate the average over the whole series of  $x$ . It can be seen all the temporal autocorrelations are short-ranged.

Fig. 6 shows the cross-correlation

$$c_{x,y}(\tau) = \frac{\langle x(t)y(t+\tau) \rangle - \langle x(t) \rangle \langle y(t) \rangle}{\sqrt{\langle x^2(t) \rangle - \langle x(t) \rangle^2} \sqrt{\langle y^2(t) \rangle - \langle y(t) \rangle^2}}$$

between density and flow rate. The cross-cor-

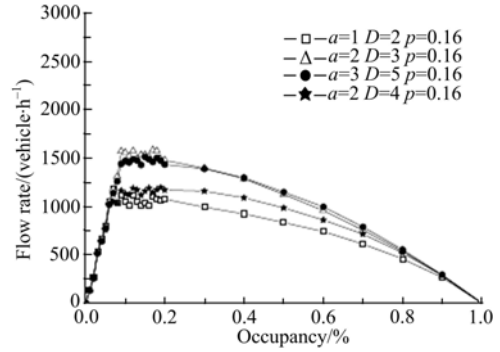


**Fig. 3** Fundamental diagrams with parameters  $a < D$ . The road length  $L = 30$  km (20000 cells).

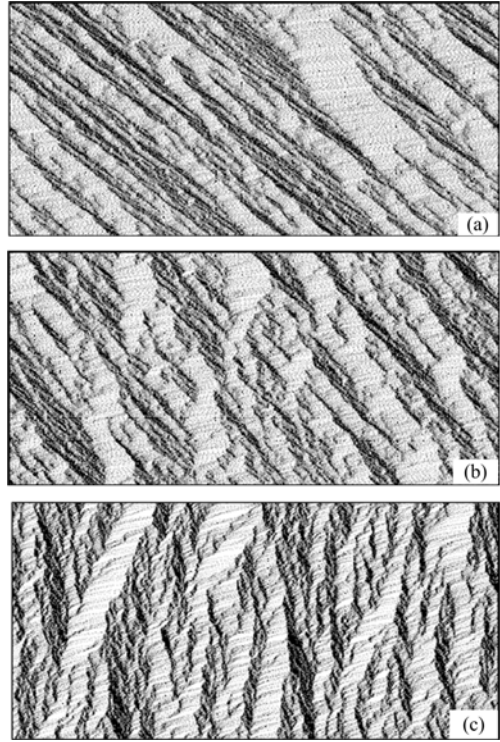


**Fig. 4** Spatiotemporal patterns at density  $\rho=0.3$  at different values of  $a$  and  $D$  with  $a < D$ . The road length  $L = 7.5$  km (5000 cells). The randomization  $p=0.16$ . (a)  $a=4, D=5$ ; (b)  $a=3, D=5$ ; (c)  $a=1, D=3$ .

relation vanishes in large time scale.

### 3 Traffic patterns induced by isolated on-ramp bottleneck

This section investigates the spatiotemporal patterns induced by an on-ramp on an open road section. In order to reproduce wide moving jams, a slow-to-start rule is considered by assuming a variable randomization

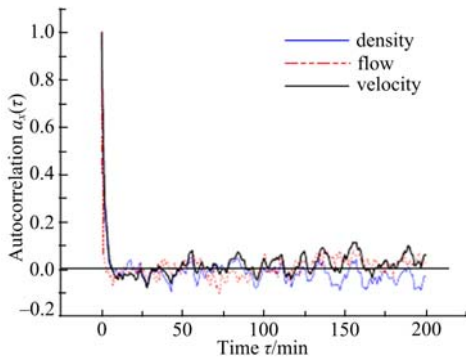


Fig. 5 Autocorrelation functions of local density, average velocity and flow rate in congested state. The parameters are the same as that in Fig. 4(b).

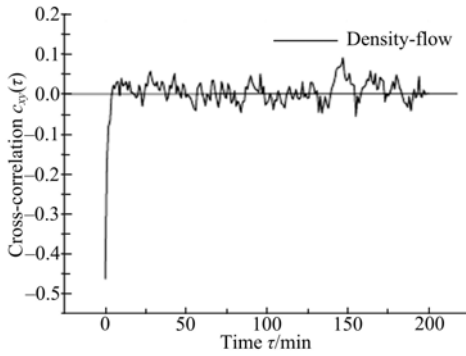


Fig. 6 Cross-correlation functions between local density and flow rate in congested state. The parameters are the same as that in Fig. 4(b).

probability

$$p = \begin{cases} p_0 & \text{if } t_{s,n} \geq t_c \\ p_d & \text{if } t_{s,n} < t_c \end{cases}$$

Here  $t_{s,n}$  is the stopped time of vehicle  $n$ . The open boundary conditions are set as follows. Assuming the left-most cell on the road corresponds to  $x=1$ , at each time step, a new vehicle will be injected from the position  $x=5$  with probability  $p_{in}$  provided  $x_{last} \geq 10$ . Here  $x_{last}$  denote the position of the last vehicle on the road. The velocity of the inserted vehicle is set to  $\min(v_{max}, d)$ .  $d$  is the space gap in front of the new vehicle. The stop time  $t_{s,n}$  of the newly injected vehicle is set to 0. At the right boundary, the leading vehicle moves without any hindrance. When the position of the leading vehicle  $x_{lead} > L$ , in which  $L$  corresponds to the position of the exit, it will be

removed and the second vehicle becomes the leader.

The on-ramp bottleneck is fulfilled as follows. At each time step, the merging region will be scanned from downstream to upstream. The longest space gap will be selected, and if the space is larger than  $L_v$  (5 cells), a new vehicle will be inserted into the middle of the space with probability  $p_{on}$ . The velocity of the inserted vehicle is set to  $\min(v_{max}, d)$ . Here  $d$  denotes the space gap in front of the new vehicle. The stop time  $t_{s,n}$  of the newly injected vehicle is set to zero.

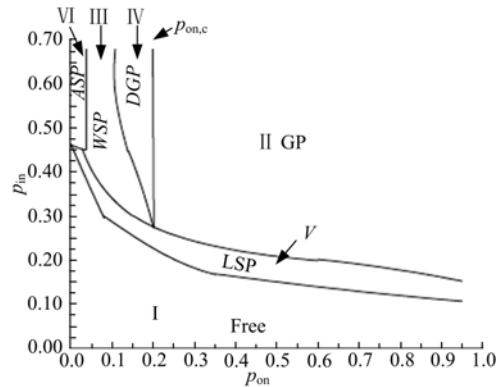
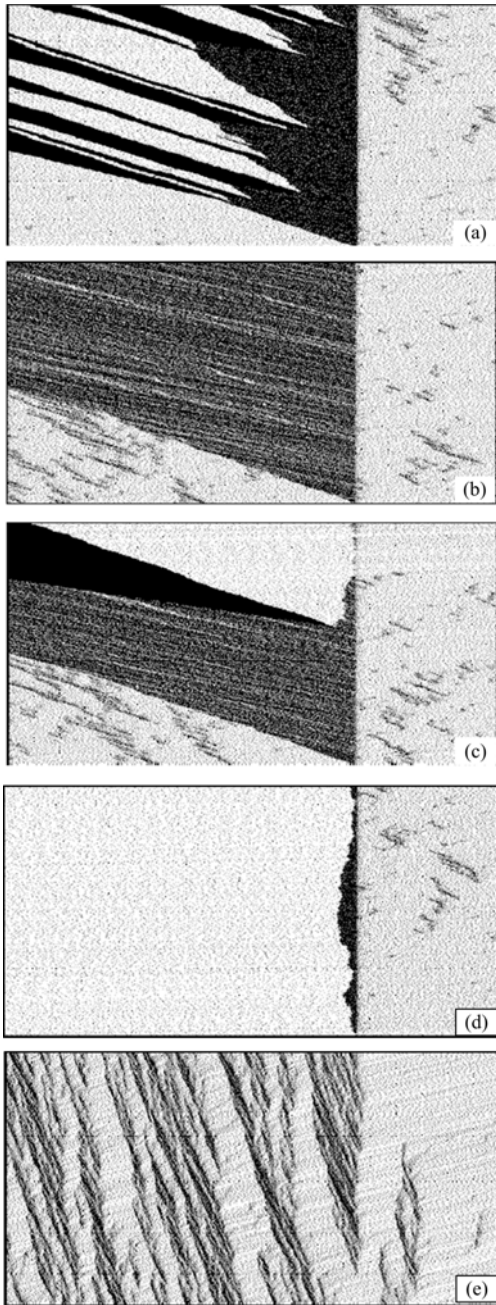


Fig. 7 Pattern diagram in the space of  $(p_{on}, p_{in})$

Fig. 7 shows the pattern diagrams in the space of  $(p_{on}, p_{in})$ . The space is divided into six regions. In region I, free flow exists on the whole road. In region II, the congested pattern is named “general pattern” (GP) [10], in which synchronized flow appears upstream of merging region and wide moving jams spontaneously emerge in the synchronized flow. In the GP, synchronized flows are bounded by a sequence of wide moving jams. The downstream fronts of the jams move upstream with a constant speed. The region of GP is continuously widening upstream. Spatial-temporal features of GP are shown in Fig. 8(a).

In region III, where  $p_{on}$  is not so large, wide moving jams do not emerge in synchronized flow. There is only synchronized flow upstream the merging region. The downstream front of the synchronized flow is fixed at the merging region and the upstream front



**Fig. 8** The space-time plots of the congested patterns. (a) GP (b)WSP (c)DGP (d)LSP (e)ASP. In (a)  $p_{in}=0.4$ ,  $p_{on}=0.6$ ; (b)  $p_{in}=0.6$ ,  $p_{on}=0.15$ ; (c)  $p_{in}=0.6$ ,  $p_{on}=0.14$ ; (d)  $p_{in}=0.2$ ,  $p_{on}=0.4$ ; (e)  $p_{in}=0.6$ ,  $p_{on}=0.02$ ; The cars are moving from the left to the right, and the vertical direction(up) is (increasing) time. The vertical direction corresponds to 10000 time steps in (a) - (d), 1000 time steps in (e).

is continuously widening upstream. This pattern is named the “widening synchronized flow pattern”(WSP)<sup>[10]</sup> as shown in Fig. 8(b). Fig. 9

shows the one minute averaged flow rate-density data obtained by a virtual detector at  $x=9$  km(i.e., the 6000 th cell). The data is widely scattered in a 2D dimension, which is consistent with empirical observations.

In region IV, which is between WSP and GP, the “dissolving general pattern”(DGP)<sup>[10]</sup> occurs. In this pattern, the transition from synchronized flow to jams occurs inside the WSP. But it could not induce wide moving jams sequences, as Fig. 8(c) shows. This is because the outflow rate of the jam is smaller than the capacity of the merging region. As a result, free flow occurs between the merging region and the downstream front of the jam. The boundary between regions II and IV is a vertical line with the coordinate  $p_{on}=p_{on,c}$ . Upon this boundary, the capacity of the merging region equals to the outflow rate of the jams.

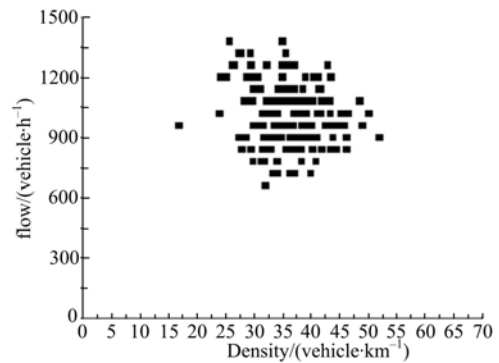


**Fig. 9** The one minute averaged flow rate-density data observed by a virtual detector at the 6000 th cell. The corresponding traffic pattern is shown in Fig. 8(b).

In region V, the upstream front of the synchronized flow is not continuously widening over time, but limited somewhere upstream of the merging region. The whole synchronized region is localized. So this pattern is called the “localized synchronized flow pattern”(LSP)<sup>[10]</sup>. Spatial-temporal features of LSP are shown in Fig. 8(d).

Finally, in region VI where  $p_{in}$  is large and  $p_{on}$  is very small, a spatially mixture of free flow and synchronized flow appears on

the road as shown in Fig. 8(e). At a fixed position on the road, one will observe alternative regions of free flow and synchronized flow. Therefore, it is called “SP with alternations of free and synchronized flow” (ASP)<sup>[10]</sup>.

As in other works, it should be noted that the boundaries in Fig. 7 are not so rigorous. Especially near the boundary between regions III and IV, both WSP and DGP could occur under the same set of parameters. Different random seeds could exhibit different patterns.

The pattern diagram in Fig. 7 and the spatial-temporal patterns in Fig. 8 are all qualitatively consistent with the well-known results of the three-phase traffic theory<sup>[10]</sup>. Therefore, we believe the synchronized flow is reproduced by the refined NaSch model with  $a < D$ .

#### 4 Conclusion and discussion

This paper studies the effect of acceleration  $a$  and randomization  $D$  in the refined NaSch model. It is found the value of  $a/D$  plays an important role in the traffic dynamics. When  $a/D \geq 1$ , the fundamental diagrams and spatiotemporal diagrams are qualitatively unaltered. In contrast, when  $a/D < 1$ , a qualitative change of traffic characteristics happens with the decrease of  $a/D$ . It is found the congested traffic might be related to synchronized flow through correlation analysis.

We also study the traffic patterns induced by an isolated on-ramp on an open road section by using the refined model with  $a/D < 1$  and by considering slow-to-start rule. It is shown the traffic patterns are in well consistency with the results of three phase theory. Therefore, we believe the synchronized flow is reproduced by the refined NaSch model.

Our work is expected to shed some light on the mechanism of synchronized flow. Pre-

vious studies have proposed many mechanisms to explain synchronized flow. Our work indicates the synchronized flow might be relevant to the ratio of  $a/D$ . Of course, further investigations are needed in this field in future work.

Finally, we would like to mention more works on the refined NaSch model is needed to reproduce, e. g., first order phase transition from free flow to synchronized flow, as well as the moving synchronized pattern.

#### 参考文献:

- [ 1 ] Lighthill M J, Whitham G B. On kinetic waves: II. A theory of traffic flow on long crowded roads[J]. Proc Roy Soc Lon, Ser A, 1955, 229:317-345.
- [ 2 ] Raney B, Voellmy A, Cetin N, et al. Towards a microscopic traffic simulation of all of Switzerland[J]. Lecture Notes in Computer Science, 2002, 2329:371-380.
- [ 3 ] Nagel K, Rickert M. Parallel implementation of the TRANSIMS micro-simulation[J]. Parallel Computing, 2001, 27 (12): 1611-1639.
- [ 4 ] Cetin N, Nagel K, Raney B, et al. Large-scale multi-agent transportation simulations[J]. Computer Physics Communications, 2002, 147(1/2): 559-564.
- [ 5 ] Nagel K, Schreckenberg M. A cellular automaton model for freeway traffic[J]. J Phys I (France) 1992, 2: 2221-2229.
- [ 6 ] Kerner B S, Rehborn H, Aleksic M, et al. Recognition and tracking of spatial-temporal congested traffic patterns on freeways[J]. Transportation Research Part C, 2004, 12 (5): 369-400.
- [ 7 ] Kerner B S. Control of spatiotemporal congested traffic patterns at highway bottlenecks[J]. IEEE Trans ITS, 2007, 8(2): 308-320.
- [ 8 ] Knospe W, Santen L, Schadschneider A, et al. Single-vehicle data of highway traffic: Microscopic description of traffic phases[J]. Phys Rev E, 2002, 65: 056133.
- [ 9 ] Neubert L, Santen L, Schadschneider A, et al. Single-vehicle data of highway traffic: A statistical analysis [J]. Phys Rev E, 1999, 60:6480-6490.
- [10] Kerner B S. The Physics of Traffic [M]. Berlin: Springer, 2004.